# EFFECTS OF SALT FREEZE DAMAGE ON THE VISCOELASTIC PERFORMANCE OF ASPHALT MORTAR

#YANAN CUI*, **, DONGSHENG CHEN**, LEI FENG**, LE WANG**

*The Key Laboratory of Road Structure & Material Ministry of Transport,
Haidian District Xitucheng Road No. 8, Beijing, PRC
**College of Civil Engineering, Inner Mongolia University of Technology,
Ai Min Road No. 49, Xin Cheng District, Hohhot, Inner Mongolia, PRC

#E-mail: yanancui@aliyun.com

*In cold regions, road pavements are frequently covered by ice and snow because of low temperatures and extreme weather conditions during winter. Deicing salt is commonly used to reduce icing coverage and clean pavements. However, the repetitive use of deicing salt may have a negative impact on the pavements that are made from a mixture of asphalt mortar and coarse aggregate. This paper discusses the viscoelastic behavior of asphalt mortar in salt freezing environments. The study consists of three steps. First, uniaxial creep tests are conducted on asphalt mortar specimens under different freeze-thaw cycles. Then, a Burgers model with a damage factor is proposed in order to obtain the viscoelastic parameters. Finally, scanning electron microscopy (SEM) is used to study the microstructure of asphalt mortar and to investigate the structural changes that take place during freeze-thaw cycles. The results of the study indicated that freeze-thaw cycles with different salt concentrations can damage asphalt mortar and change its viscoelastic properties. The Burgers damage model is shown to reflect the creep of asphalt mortar more accurately than the Burgers model. From the results, it can be concluded that it is necessary for cold regions to control vehicle overloading and limit the amount of deicing salt to be used on pavement.*

## INTRODUCTION

In cold regions it is crucial to improve the frost resistance of asphalt concrete in order to improve pavement durability [1-2]. Many cold regions are facing problems that may adversely affect the proper use of salt on roads in winter, including aging, decreases in the number of operators and cuts in the budget for road maintenance [3-4]. To ensure proper performance and durability of asphalt pavement, it is necessary to study its behavior under conditions that are similar to what it experiences in the field.

Asphalt concrete is a multiphase material that is composed of asphalt, aggregate, and voids [5-6]. For this reason, its formation mechanism is very complex. From the viewpoint of multiphase theory, asphalt mixtures can be regarded as mixtures composed on three levels. The first level is an asphalt binder consisting of asphalt and mineral powder. The asphalt binder is the major bonding element of the mixture, and it must be stable in water and other severe conditions while having sufficient cohesion. If this component is unstable, various types of distress can occur in asphalt pavements [7-8]. The second level is the asphalt mortar, which is composed of asphaltine and fine aggregate. The asphalt mortar has higher strength and better resistance to shrinkage than the asphaltine itself. The third level is a stable mixture in which coarse aggregate particles form a solid skeleton and the asphalt mortar fills the space between the particles. The strength of the asphalt mixture mainly depends on the binding effect of the asphalt mortar and the skeleton of the coarse aggregate.

As mentioned above, asphalt mortar is a mixture of fine aggregate (d < 4.75 mm) and asphaltine [9], i.e. a mixture in which fine aggregates are dispersed in the asphalt phase [10] (similar to the mixture of sand and cement in cement mortar). Within the field of asphalt concrete technology, many researchers are interested in the performance of asphalt mortar under different exposure conditions. Cai [11] performed uniaxial creep tests under different stress levels and temperatures to investigate the behavior of asphalt mortar under both short- and long-term loading. The functional relationships between the creep model parameters, temperature and stress were obtained by correlation analysis. The influence of the creep model parameters on the creep performance of asphalt mortar was also investigated.

Asphalt mortar generally has high viscosity and ductility, but if the viscosity and ductility are too high, the stability of the asphalt concrete is reduced. This can

result in such problems as high air void content, non-uniform mixture and difficult compaction. All of these factors are considered to be major contributing factors to the premature failure of asphalt pavement [12-13]. Therefore, it is important to achieve an accurate understanding of the performance of asphalt mortar and, especially, its mechanical properties under prescribed conditions.

Many researchers have investigated the creep behavior of asphalt concrete and mortar [8-10], but research on the creep behavior of salt-contaminated asphalt mortar is relatively rare. In order to fill this gap, this paper focuses on the study of the creep behavior of salt-contaminated asphalt mortar. In this paper, uniaxial creep tests were performed on styrene-butadiene-styrene (SBS) modified asphalt mortar specimens after they had been exposed to freeze-thaw cycles. Also, the impact of freeze-thaw cycling and salt solutions on the elastic and viscoelastic behavior of the test specimens are investigated. Furthermore, a modified Burgers model was fitted to the measured experimental data and the model parameters were obtained. Finally, scanning electron microscopy (SEM) was used to investigate the changes to the microstructure of asphalt mortar after freezing and thawing.

## EXPERIMENTAL

### Material properties

In this study, 48 groups of asphalt samples were prepared with diameter 101.6 mm and length 63.5 mm according to the T 0702-2011 Marshall method (Standard Test Methods of Bitumen and Bituminous Mixtures for Highway Engineering JTG E20-2011) [14]. The basic physical properties of the asphalt mortar samples are given in Tables 1 and 2.

*Asphalt.* In this study, SBS modified asphalt was used as the binder for the asphalt mortar. Table 1 shows the technical parameters of the asphalt. All of the physical properties of the asphalt mortar samples are listed and identified by their test norm numbers. These data were collected according to the Standard Test Methods of Bitumen and Bituminous Mixtures for Highway Engineering [14].

*Mix ratio.* Successful asphalt mortar has an aggregate that is clean, rigid, abrasion resistant, free of acidic minerals, and consists of 100 % fractured surfaces. The asphalt mortar used in this study consisted of fine aggregates, mineral and asphalt in the mix ratio shown in Table 2. The mix proportion of the asphalt mortar is converted from the dense gradation asphalt mixture ratio of AC-16, which conforms to the Chinese standard Technical Specifications for construction of Highway Asphalt Pavements JTG F40-2004 [15] by the Specific Surface Area change algorithm [9].



Figure 1.  Core specimens of asphalt mortar.

Table 2.  Mix proportion of asphalt mortar.

| Ingredient | | Mass percentage |
|---|---|---|
| Fine aggregate size (mm) | 0 ~ 0.075 | 10.45 % |
| | 0.075 ~ 0.15 | 0.65 % |
| | 0.15 ~ 0.3 | 0.48 % |
| | 0.3 ~ 0.6 | 3.74 % |
| Mineral aggregate | | 10.92 % |
| asphalt | | 8.96 % |

Table 1.  Technical parameters of SBS modified asphalt.

| Test items | Required | Measured | Test Norm |
|---|---|---|---|
| Penetration degree (25°C, 5 s, 100 g) (0.1 mm) | 60 ~ 80 | 65 | T0604 |
| PI (penetration index) | $\geq$ -0.4 | -0.2 | T0604 |
| Ductility (5°C, 5 cm·min$^{-1}$) (cm) | $\geq$ 30 | 33 | T0605 |
| Softening point (°C) | $\geq$ 55 | 62 | T0606 |
| Relative density (25°C) | – | 1.02 | T0603 |
| Kinematic viscosity (mm$^2$·s$^{-1}$) | $\leq$ 3 | 1.19 | T0625 |
| Flash point (°C) | $\geq$ 230 | 269 | T0611 |
| Segregation (°C) | $\leq$ 2.5 | 1.1 | T0661 |
| RTFOT (rolling thin film oven test) residue | | | T0610 |
| Quality change (%) | $\leq$ ±1.0 | 0.242 | T0610 |
| Penetration ratio (%) | $\geq$ 60 | 67.0 | T0604 |
| Ductility (5°C, 5 cm·min$^{-1}$) (cm) | $\geq$ 20 | 23 | T0605 |

*Test specimens.* The test asphalt mortar specimens (Figure 1) were cored from Marshall specimens [14] with 38 mm diameter and 62 mm height.

Table 3. Deicing salt composition.

| Chemical compound | Mass percentage (%) | CAS (Chemical Abstracts Service) No. |
|---|---|---|
| CaCl₂ | ~ 51.0-51.5 | 7774-34-7 |
| NaCl | ~ 43.5-44.0 | 7647-14-5 |
| MgCl₂ | ~ 3.0-3.2 | / |
| Other | ~ 1.8-2.0 | / |

*Deicing salt composition.* In this study, a calcium chloride-based deicing salt was used for the tests (see Table 3). This salt is widely used in cold regions.

### Freeze-thaw test

In order to investigate the creep performance of SBS-modified asphalt mortar that has been exposed to low temperature and a deicing salt environment, four different salt concentrations (0, 2 %, 4 %, and 6 %) and four different numbers of freeze-thaw cycles (3, 8, 15, and 25) were used. Because the asphalt mortar specimens were small and the core temperature reached the test temperature in a relatively short time, the frost resistance method of cement concrete (freezing method) was used with a freeze-thaw temperature cycle from -20°C to 20°C. The specimens were first soaked in a water or salt solution for 4 days, frozen at -20°C for 2 hours and then thawed at 20°C for 2 hours. The same procedures were repeated for 3, 8, 15, or 25 cycles to simulate realistic deicing freeze conditions. Figure 2 shows the test specimens in the freeze-thaw tank.



Figure 2. The test specimens in the freeze-thaw tank.

### Uniaxial creep test

Uniaxial creep tests were conducted using a U.S. GCTS triaxial compression apparatus (Figure 3) at a test temperature of 20°C. Three different axial compression values (300 kPa, 500 kPa and 700 kPa, respectively) were applied to each group of specimens. First, a prestress of 5 kPa was exerted on the specimen for 1 min. Subsequently, the desired stress was applied and maintained either for 90 minutes or until a 5 % axial strain was reached.
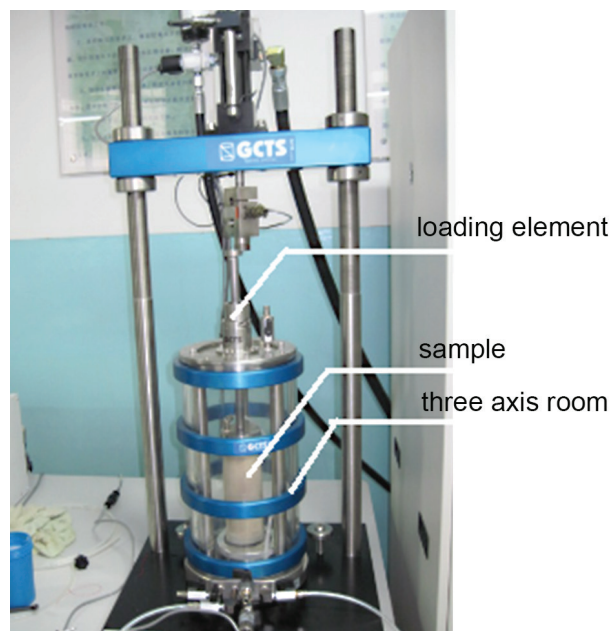


Figure 3. U.S. GCTS Triaxial Compression Apparatus.

### SEM investigation

The microstructural changes of the asphalt mortar after different salt freeze cycles were observed by scanning electron microscopy (SEM Hitachi S-3400N, Japan).

## RESULTS AND DISCUSSION

### Microstructure investigation

Figure 4 shows the SEM images of the microstructures of typical test specimens that were subjected to different freeze-thaw cycles in water or salt solution and subsequently subjected to creep tests.

Figure 4 shows that as the salt solution concentration, number of freeze-thaw cycles, and axial stress increased, the adhesion between asphalt and aggregate became increasingly destroyed, interface cracks became wider, and the number of cracks significantly increased. The integrity of the aggregate particles was damaged. Some particles even broke up into powder, causing the microstructure of the asphalt to become loose. There are several possible explanations for this phenomenon: (1) during the process of freezing and melting, asphalt and aggregate experienced incompatible deformations due to the difference in their thermal expansion coefficients, which could cause interface cracks; (2) when

the temperature decreased, the water in the mortar voids froze and led to expansion stress, causing the salt solution to migrate and permeate the asphalt-aggregate interface faster and crystallize with a crystal expansion effect during alternate freezing and thawing, thus accumulating damage and destroying the structure of the asphalt mortar; (3) the salt solution may have damaged the adhesion between the asphalt and the aggregate and affected the interfacial compatibility between them; (4)

for identical salt solution concentrations and freeze-thaw cycles, the microstructure of the asphalt became looser and the number of cracks increased when the axial compression increased.

Creep tests

In order to reveal the combined effects of freeze-thaw cycles and load exposure to asphalt mortar, a comparative analysis of creep test results was performed.
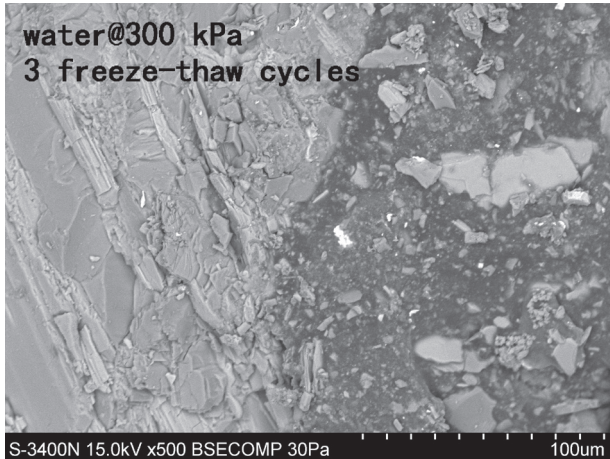


a) 3 freeze-thaw cycles
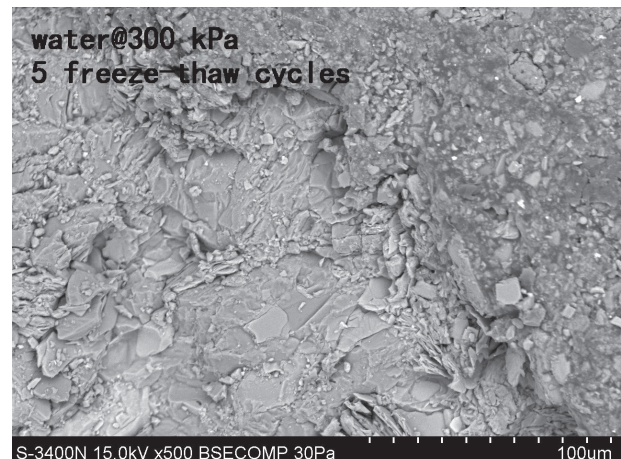
b) 5 freeze-thaw cycles

c) 300 kPa
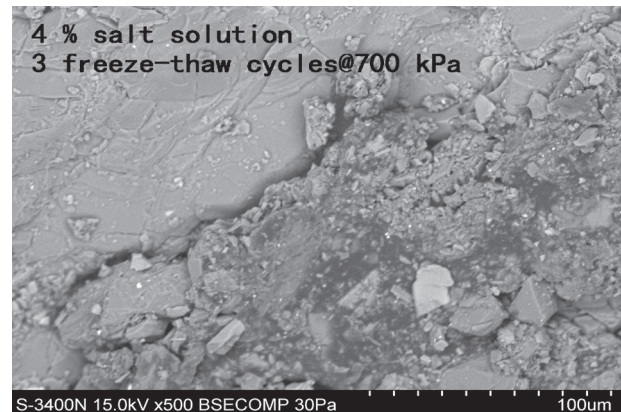
d) 700 kPa

e) 2 % salt
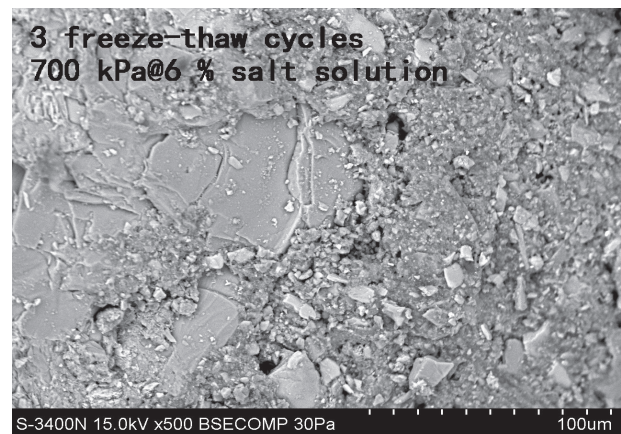
f) 6 % salt

Figure 4. SEM images of the microstructure of asphalt mortar after exposure to: a) 3 and b) 5 freeze-thaw cycles, axial compressive stresses of c) 300 kPa and d) 700 kPa, and salt solution concentrations of e) 2 % and f) 6 %.

As Figure 5 shows, a typical tensile creep curve (as in curve 1) can generally be divided into three phases: creep migration, creep stability and creep failure. For compressive creep (as in curve 2), the latter section (creep failure) is usually missing. The first phase is generally a period of rapid creep. In compressive creep (curve 2), this could also be named the "material compaction phase" due to the applied load because the material porosity decreases rapidly, resulting in a compaction of the specimens and the resulting occurrence of large strains. In the second phase, the creep rate (deformation rate) attains a constant value (stable creep phase, also known as the steady creep phase). The third phase is the period of destructive creep, characterized by asphalt mixture structure damage and loss of strength. In this phase, also called the accelerated creep phase, the deformation increases rapidly, resulting in the failure of the whole specimen [16]. Due to the limitations of the applied load and the test time, compressive creep usually only occurs in the first two phases (creep migration and creep stability), a finding that is further confirmed by the following test results.
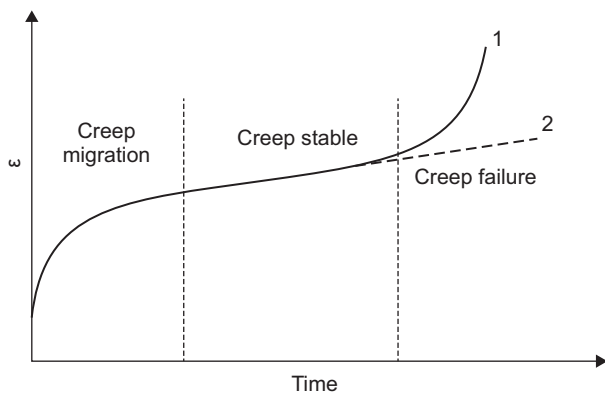


Figure 5. Typical 1 tensile and 2 compressive creep curves of asphalt mixtures.

### Effect of axial compression

Figure 6 shows that under different salt solution concentration conditions, the creep curves exhibit both creep migration and the steady creep phase. Additionally, as the axial compression increases, the strain more closely corresponds to steady creep. Since the slope of the steady creep phase reflects the creep rate, i.e. the rate of strain or deformation, the strain of the asphalt mortar grows most rapidly when the axial compression is at its highest value (here 700 kPa).

### Effect of salt solution concentration

Figure 7 shows the creep curves of the specimens in different salt solution concentrations. Whether the sample was subjected to 15 or 25 freeze-thaw cycles, the samples tested with pure water exhibited the highest strain. This is because the water in the mortar voids will freeze when the temperature is below 0°C, leading to increased volume and ice pressure; when the temperature rises, the ice melts, and after repeated freezing and thawing the damage accumulates. As a result, the structure of the asphalt mortar is destroyed and its strength is reduced.

Compared to pure water, the salt solution migration and permeation in the gaps of asphalt mortar makes $Ca^{2+}$ ions adsorbed at the asphalt-aggregate interfaces to generate insoluble material, resulting in an increase in interface strength. However, salt solutions with different concentrations result in different effects on the asphalt mortar.

When the temperature is reduced, the salt solution with the low concentration (2 %) tends to freeze easily because of its relatively high freezing point, resulting in ice pressure in the specimen voids. The salt solution with the high concentration (6 %) has a lower freezing point and is not easily frozen. On the other hand, the internal moisture will migrate when the water in the gaps near the surface of the specimen freezes. Thus, the
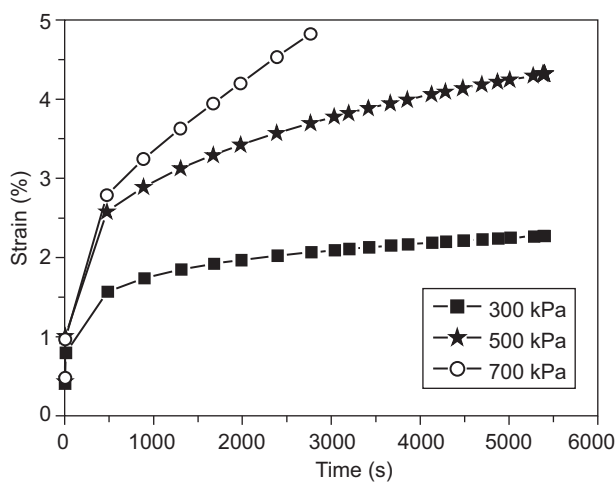


a) 25 freeze-thaw cycles
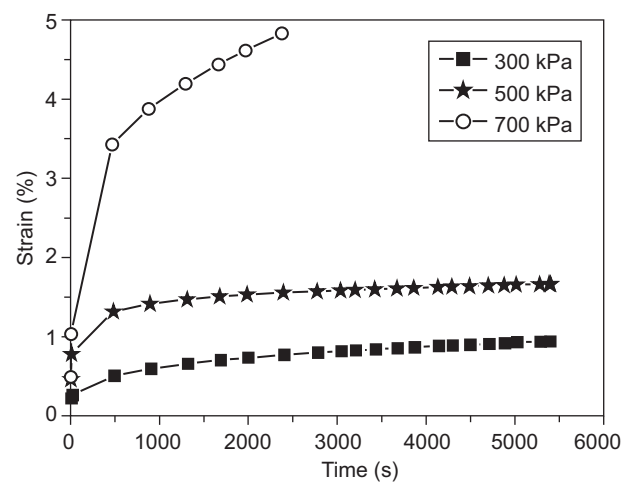


b) 15 freeze-thaw cycles

Figure 6. Creep curves under different axial compression loads after (a) 25 freeze-thaw cycles in water and (b) 15 freeze-thaw cycles in 4 % salt solution.

salt concentration in the gap of the specimen interior reaches saturation conditions more easily, resulting in crystallization and crystal expansion pressure within the small volume of asphalt mortar voids. The salt solution with the intermediate concentration (4 %) attained a balance between these two counteracting effects. As the temperature in this sample decreases, the resulting freezing pressure is not significant; on the other hand, as the temperature in this sample increases, the resulting crystallization degree is not high, and does not lead to internal crack development. Thus, the deformation of the specimen under axial pressure is small.

### Effect of freeze-thaw cycles

Figure 8 shows the influence of the number of freeze-thaw cycles on the specimens, all other conditions being the same. As the number of freeze-thaw cycles increases,

preexisting small pores, cracks and other weak parts of the microstructure inside the specimen are affected by ice expansion so that the void space becomes more connected and its volume fraction increases, leading to structural damage and a decrease in strength. Therefore, as the number of freeze-thaw cycles increases, the internal damage within the asphalt mortar also increases, causing the performance to gradually deteriorate. After 25 freeze-thaw cycles, the creep curves tend toward creep failure (see Figure 8b).

### Modeling of the results by a viscoelastic constitutive model of asphalt mortar

In order to describe the viscoelastic behavior of asphalt mortar, a suitable mechanical model has to be chosen. The Burgers model, which employs the Maxwell



a) 15 freeze-thaw cycles  b) 25 freeze-thaw cycles
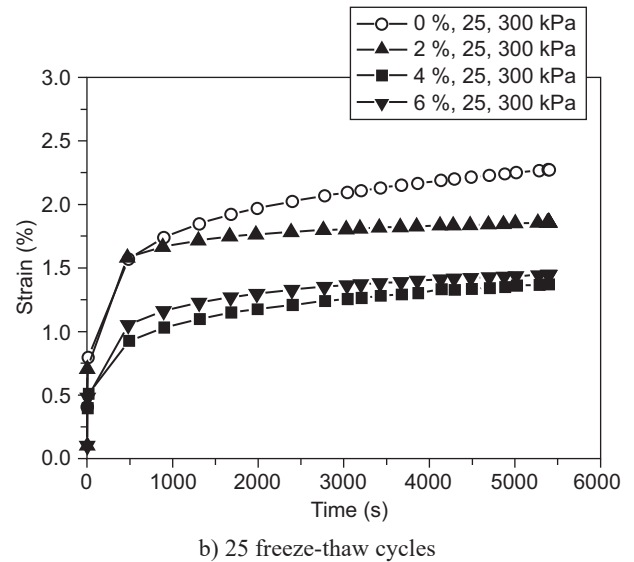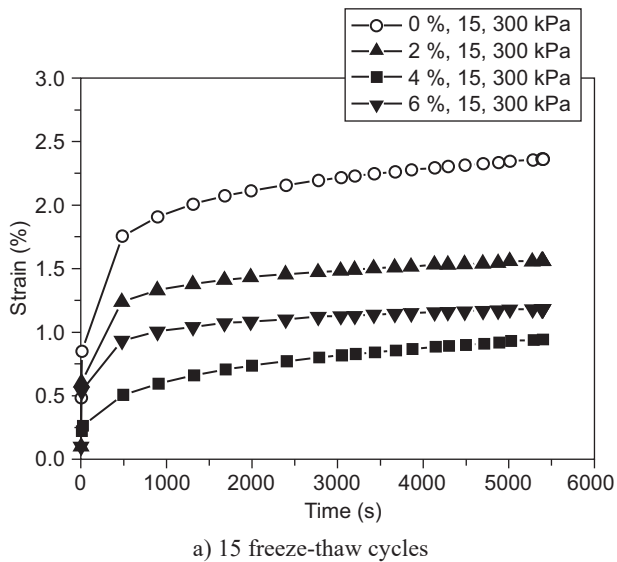
Figure 7. Creep curves under an axial compression load of 300 kPa and different salt solution concentrations after (a) 15 and (b) 25 freeze-thaw cycles.



a) 6 % salt solutions  b) 2 % salt solutions
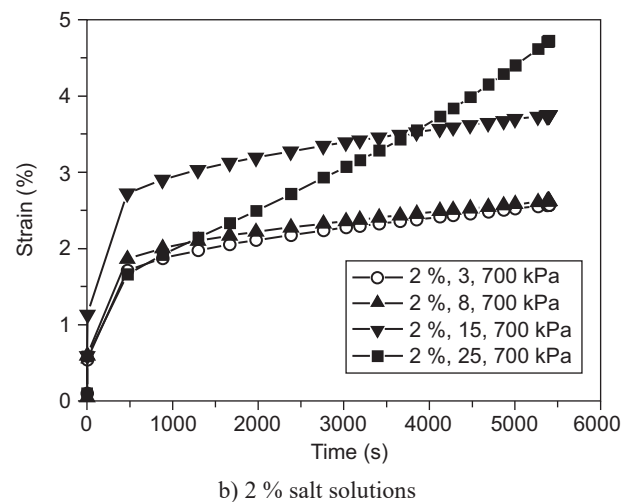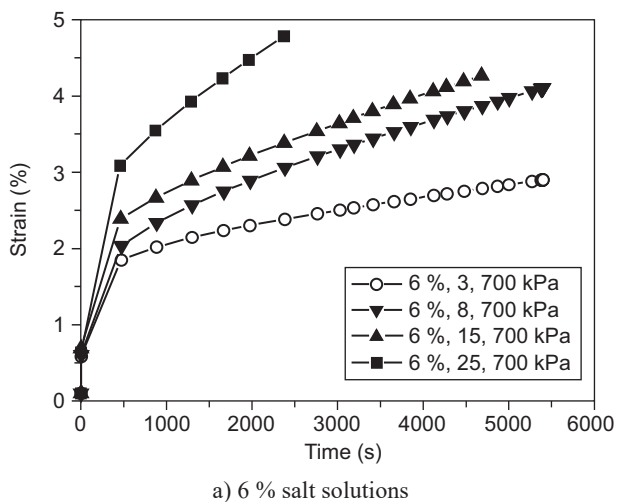
Figure 8. Creep curves for specimens under an axial compression load of 700 kPa and different numbers of freeze-thaw cycles for 6 % salt solutions (a) and 2 % salt solutions (b).

and Kelvin models with the appropriate number of parameters (see Figure 9), can successfully simulate the stress–strain characteristics of asphalt and asphalt mixtures at medium and low temperatures [17-18]. Therefore, it will be utilized in this study to imitate the creep behavior of the specimens tested.
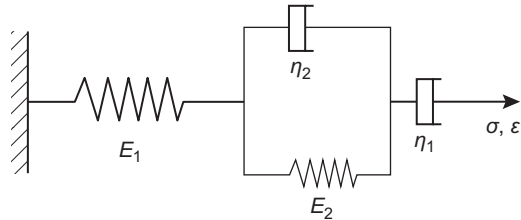


Figure 9. Burgers model.

### Burgers model with damage

The constitutive equation of the Burgers model can be written as:

$$\sigma + p_1\dot{\sigma} + p_1\ddot{\sigma} = q_1\dot{\varepsilon} + q_1\ddot{\varepsilon}, \tag{1}$$

$$p_1 = \eta_1/E_1 + (\eta_1 + \eta_2)/E_2, \tag{2a}$$

$$p_2 = \eta_1\eta_2/E_1E_2, \tag{2b}$$

$$q_1 = \eta_1, \tag{2c}$$

$$q_2 = \eta_1\eta_2/E_2, \tag{2d}$$

where $\sigma$ and $\varepsilon$ are the stress and strain and the dot superscripts represent the time derivative of the quantity involved. Coefficients $p_1$, $p_2$, $q_1$ and $q_2$ are dependent on the material properties, which are $E_1$, $E_2$, $\eta_1$ and $\eta_2$, respectively. $E_1$ and $E_2$ are the elastic moduli of the springs in Figure 9 and $\eta_1$ and $\eta_2$ are the viscosities of the corresponding dashpots.

The stress and strain of the asphalt mortar in the creep test can be written as:

$$\sigma(t) = \sigma_0 H(t) \tag{3a}$$

and

$$\varepsilon(t) = J(t)\sigma_0, \tag{3b}$$

where $H(t)$ is the function of the stress change in the creep test. In a simple creep test with constant loading, $\sigma(t)$ is equal to $\sigma_0$ and $J(t)$ is termed creep compliance, which represents the strain value under the action of a unit stress at time $t$. The compliance can be written in its expanded form as [19]:

$$J(t) = \frac{1}{E_1} + \frac{t}{\eta_1} + \frac{1}{E_2}\left(1 - \exp\left(-\frac{t}{\tau}\right)\right) \tag{4}$$

where $\tau = \eta_1\eta_2/E_2$. In the following, the experimental data obtained in this work will be utilized to determine the four parameters ($E_1$, $E_2$, $\eta_1$ and $\eta_2$) of the Burgers

model. Once the model is thus calibrated, it is expected to accurately represent the basic features of the creep behavior of asphalt mortal subjected to freeze-thaw action with or without concurrent exposure to a salt solution.

Under the action of external loads and freeze-thaw cycles in salt solutions, the material will be damaged by structural defects such as cracks and pitholes. In the continuum damage mechanics framework [20], damage variables can be used to describe the effects of damage on the material. In the context of damage analysis of rock or concrete materials, it has been shown [21] that the Weibull distribution is suitable to describe the damage and fracture process of such materials.

Therefore, it is possible to use the three-parameter Weibull function to describe the defect distribution of asphalt mortar:

$$f(t) = \frac{m}{n}(t - \gamma)^{m-1}\exp\left(-\frac{(t - \gamma)^m}{n}\right) \tag{5}$$

where $m$ and $n$ are the distribution parameters and $\gamma$ is a time shift parameter (location parameter). The damage evolution equation can then be defined as:

$$\frac{dD(t)}{dt} = f(t) \tag{6}$$

where $D(t)$ is the continuous damage factor. The integrated form of Equation 6 is:

$$D(t) = \int_\gamma^t \frac{m}{n}(x - \gamma)^{m-1}\exp\left(-\frac{(x - \gamma)^m}{n}\right)dx =$$

$$= 1 - \exp\left(-\frac{(t - \gamma)^m}{n}\right) \tag{7}$$

where the location parameter $\gamma$ is equivalent to the damage threshold. For asphalt mortar, in order to simplify the analysis, one may assume that the threshold value is $\gamma = 0$, because the as-shaped specimen will already contain defects. Thus, the simplified damage factor is given by a two-parameter Weibull function:

$$D(t) = 1 - \exp\left(-\frac{t^m}{n}\right). \tag{8}$$

When the asphalt mortar sample undergoes the process of creep, damage will accompany the whole loading process. Therefore, the viscoelastic continuum damage constitutive equation can be written as:

$$\varepsilon(t) = [1 - D(t)]^{-1}\sigma_0 = \exp\left(\frac{t^m}{n}\right)\sigma_0$$

$$\left[\frac{1}{E_1} + \frac{t}{\eta_1} + \frac{1}{E_2}\left(1 - \exp\left(-\frac{t}{\tau}\right)\right)\right] \tag{9}$$

Then, the creep compliance after damage is taken into account is:

$$J'(t) = \frac{\varepsilon(t)}{\sigma_0} = \exp\left(\frac{t^m}{n}\right)\left[\frac{1}{E_1} + \frac{t}{\eta_1} + \frac{1}{E_2}\left(1 - \exp\left(-\frac{t}{\tau}\right)\right)\right]. \quad (10)$$

Figures 10 a and b show the creep test data obtained for an axial compression pressure of 300 kPa and 15 freeze-thaw cycles for 6 % and 4 % salt solutions, fitted according to Equations 4 and 10.

It is clear from the fitting results that the experimentally measured creep compliance is in excellent agreement with the Burgers damage model. As expected, fitting by the Burgers damage model (with more fit parameters) leads to closer fits than the simple Burgers model (the correlation coefficients for the Burgers model with damage were 0.9981 and 0.9968, which is superior to the values of 0.9758 and 0.9085 obtained for the simple Burgers model). Thus the fitting results provide further support to the hypothesis that material damage occurs under the action of both load and environment.

### Sensitivity analysis of the Burgers damage model parameters

The Burgers damage model parameters were obtained using non-linear fitting of the measured experimental data. Table 4 shows the fitting results for one paradigmatic example (300 kPa, 6 % salt solution, 15 freeze-thaw cycles). Sensitivity analysis was performed for the four parameters $E_1$, $E_2$, $\eta_1$ and $\eta_2$, in order to understand how these model parameters influence the creep curves. Figure 11 shows how the creep curve is affected when the elastic moduli and the viscosity coefficients are changed.

As can be seen from Figures 9 and 11a, $E_1$ is the instantaneous elastic modulus generated by the elastic element, and its deformation can be completely restored after unloading. $E_1$ influences the starting value of the creep migration phase and the absolute level of the steady creep; as the $E_1$ value increases, the creep decreases (see Figure 11a).

From Figure 11c, it is evident that the viscosity coefficient $\eta_1$ changes the slope of the steady creep phase. The greater the value of $\eta_1$, the smaller the slope of the steady creep phase. However, $\eta_1$ is the viscosity coefficient produced by residual unrecoverable deformation, see Figure 9, and it acts as the main index to evaluate resistance to permanent deformation; as its value increases, the asphalt pavement becomes more able to resist permanent deformation under loads.

$E_2$ and $\eta_2$ represent the viscoelastic effects produced over a long time under load, during which the deformation can increase gradually. $E_2$ affects the variation range of the initial creep migration phase; the larger the $E_2$ value, the larger the creep migration curvature. $\eta_2$ also affects the curvature of the creep curves, mainly in the creep migration phase (with a larger $\eta_2$ value leading to lower curvature), without significantly affecting the steady creep phase.

When the axial pressure increases, the range and slope of each creep phase will change (see Figure 6). It can therefore be concluded that the axial pressure affects each viscoelastic parameter in the model ($E_1$, $E_2$, $\eta_1$ and $\eta_2$).

When the salt concentration was changed, the steady creep phase was shifted only by a small degree, but the location and scope of the creep migration phase exhibited significant changes (see Figure 7). Therefore, it



a) 6 % salt solutions
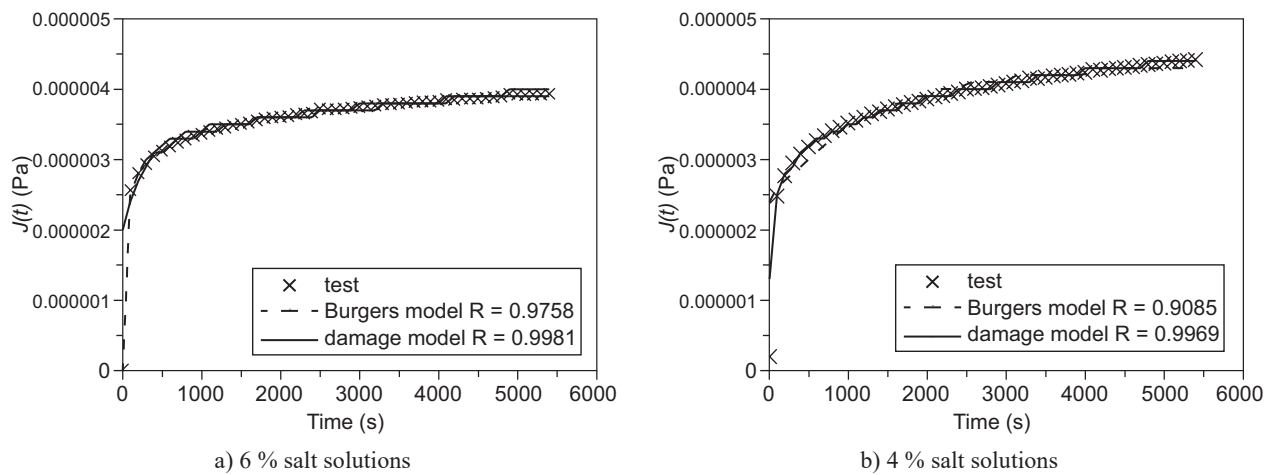


b) 4 % salt solutions

Figure 10. Creep test data for (a) 6 % and (b) 4 % salt solutions, obtained for an axial compression pressure of 300 kPa and 15 freeze-thaw cycles, fitted according to Equations 4 and 10 (Burgers model and Burgers model with damage, respectively).

Table 4. Burgers damage model parameter values (300 kPa, 6 % salt solution, 15 freeze-thaw cycles).

| Model parameter | $m$ | $n$ | $E_1$(MPa) | $E_2$ (MPa) | $\eta_1$ (GPa·s) | $\eta_2$ (GPa·s) |
|---|---|---|---|---|---|---|
| Fitting result | -11.8193 | -1.5256 | 402.972 | 1008.574 | 1100.356 | 579.663 |

can be inferred that the salt concentration in the solution mainly affects the elastic parameters $E_1$ and $E_2$.

When the number of freeze-thaw cycles was changed, the slope of the steady creep phase changed dramatically (see Figure 8), because the number of freeze-thaw cycles mainly affected the viscosity coefficient $\eta_1$.

## CONCLUSIONS

The effects of different freeze-thaw conditions on asphalt mortar were investigated by creep experiments. Based on the results of this paper, the following conclusions can be drawn:

- Salt freezing cycles have a significant influence on the viscoelastic properties of asphalt mortar. The Burgers damage model describes the creep behavior of asphalt mortar subjected to salt freezing, and the model showed that changes of the four parameters ($E_1$, $E_2$, $\eta_1$ and $\eta_{2)}$ affected every phase of the creep curve. The applied load may influence the elastic moduli as well as the viscosity coefficients occurring in the model. The salt solution concentration mainly influenced the elastic parameters, with a 4 % salt concentration having the least significant influence on the elasticity of asphalt mortar. On the other hand, the number of freeze-thaw cycles has a significant influence on the viscosity; as the number of freeze-thaw cycles increased, the viscosity of the asphalt mortar deteriorated, reducing its ability to resist deformation.

- From the micrographs of asphalt mortar, it can be seen that the asphalt mortar microstructure will be gradually destroyed by interface damage, aggregate crushing and microcrack development when the salt solution concentration, the number of freeze-thaw cycles and the axial stress are increased. This damage can influence the mechanical properties of the asphalt mortar to a great extent. Therefore, it is crucial that overloading of vehicles is avoided and that the amount of deicing salt used is strictly controlled on roads in cold areas.
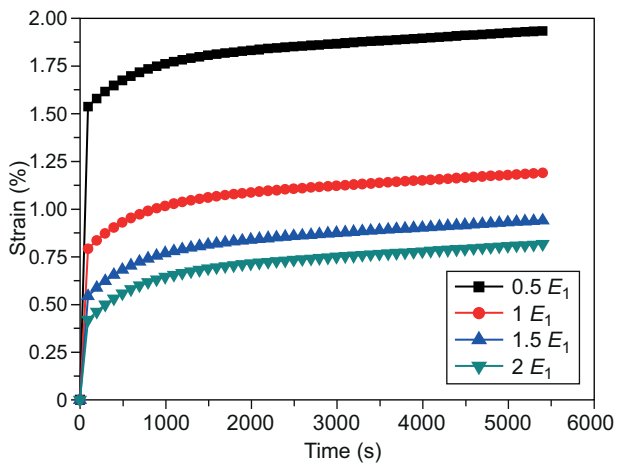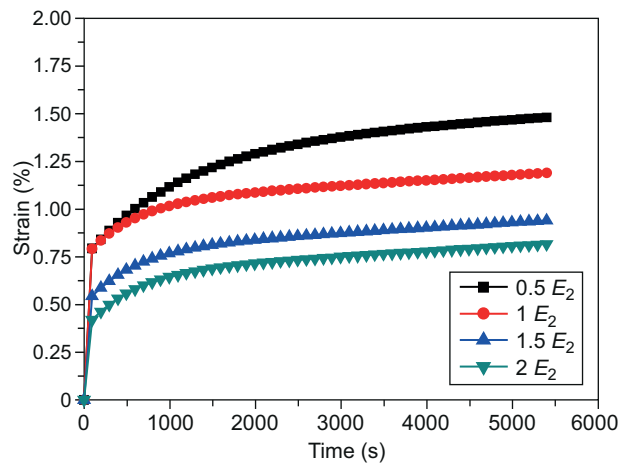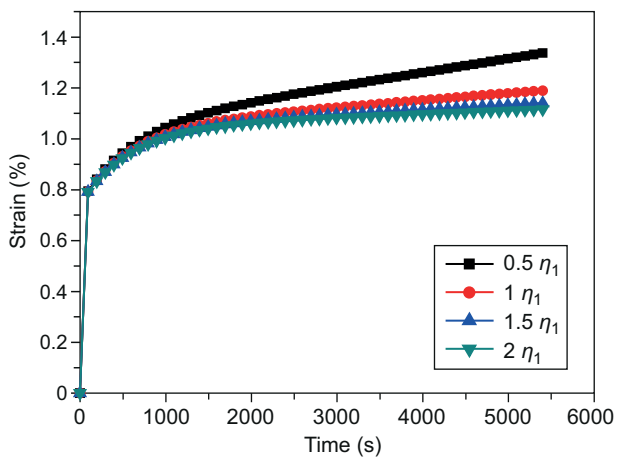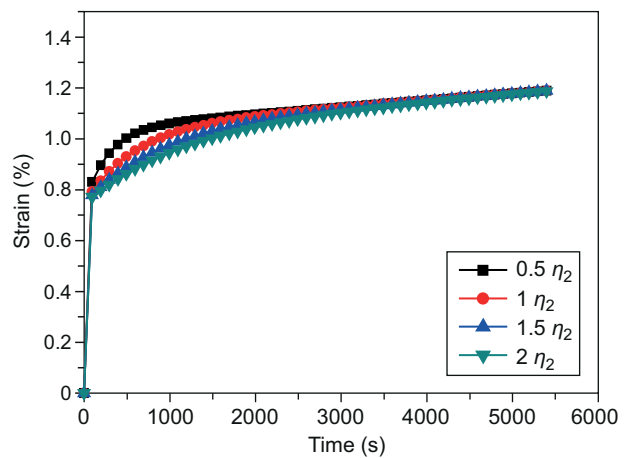


Figure 11.  Parameter sensitivity of Burgers damage model with the change of: a) elastic modulus $E_1$, b) elastic modulus $E_2$, c) viscosity coefficient $\eta_1$ and d) viscosity coefficient $\eta_2$.

Acknowledgements

REFERENCES

1. Arslan D., Guru M., Cubuk M.K. (2013): Improvement of hot mix asphalt performance in cold regions by organic-based synthetic compounds. *Cold Regions Science and Technology*, *8*, 250-255. doi:10.1016/j.coldregions.2012.09.014

2. Feng D.C., Yi J.Y., Wang D.S., Chen L.L. (2010): Impact of salt and freeze-thaw cycles on performance of mixtures in coastal frozen region of China. *Cold Regions Science and Technology*, *62*, 34-41. doi:10.1016/j.coldregions.2010.02.002

3. Ozgan E., Bektas S. (2011): An investigation of the pull-out strength of asphalt concrete exposed to varying freezing and thawing cycles. *Experimental Techniques*, *35*, 44-51. doi:10.1111/j.1747-1567.2010.00659.x

4. Fujimoto A., Tokunaga R.A., Kiriishi M., Kawabata Y., Takahashi N., Ishida T., Fukuhara T. (2014): A road surface freezing model using heat, water and salt balance and its validation by field experiments. *Cold Regions Science and Technology*, *106*, 1-10. doi:10.1016/j.coldregions.2014.06.001

5. Zhu Xing-yi, Huang Zhi-yi, Yang Zhong-xuan, Chen Wei-qiu (2010): Micromechanics-based analysis for predicting asphalt concrete modulus. *Journal of Zhejiang University-SCIENCE A (Applied Physics & Engineering)*, *11*, 415-424. doi:10.1631/jzus.A0900645

6. Ye Y.,Yang X.H., Chen C.Y. (2009): Experimental researches on visco-elastoplastic constitutive model of asphalt mastic. *Construction and Building Materials*, *23*, 316-3165. doi:10.1016/j.conbuildmat.2009.06.023

7. Norouzi A., Kim D., Kim Y. R. (2015): Numerical evaluation of pavement design parameters for the fatigue cracking and rutting performance of asphalt pavements. *Materials and Structures*, *11*, 1-16. doi:10.1617/s11527-015-0744-x

8. Zhan X.L., Lou T.L., Ming X.Y. (2013*): Effect of asphalt mortar on high-temperature properties of asphalt mixture.*

in: ICTE 2013. ASCE. pp. 2927-2932. doi:10.1061/9780784413159.423

9. Huang B T, Tian W P. (2008): Mix proportion design method of the long-term use asphalt mortar (in Chinese). *Highway*, 148-151.

10. Wu J., Yang X. H. (2014): A micromechanical framework with aggregate-mastic interaction effect for predicting uniaxial compression creep of asphalt mixture *Acta Mechanica Solid Sinica*, *27*, 306-314.

11. Cai Y. Z., Ye Y. (2010): Experimental researches on visco-elastic behavior of asphalt sand mixture (in Chinese). *Engineering Mechanics*, *27*, 200-205.

12. Wu M.M., Li R., Zhang Y.Z., Fan L., Lv Y.C., Wei J.M. (2015): Stabilizing and reinforcing effects of different fibers on asphalt mortar performance. *Petroleum Science*, *12*, 189-196. doi:10.1007/s12182-014-0011-8

13. Lira B., Jelagin D., Birgisson B. (2013): Gradation-based framework for asphalt mixture. *Materials and Structures*, *46*, 1401-1414. doi:10.1617/s11527-012-9982-3

14. Ministry of Transport (MOT) of the People's Republic of China: Standard Test Methods of Bitumen and Bituminous Mixtures for Highway Engineering (T0603, T0604, T0605, T0606, T0610, T0611, T0625, T0661, T0702), 2011-09-13.

15. Ministry of Transport (MOT) of the People's Republic of China: Technical Specifications for construction of Highway Asphalt Pavements JTG F40-2004, 2004-09-04.

16. Zeng G.W., Yang X.H., Bai F., Gao H. (2014): Visco-elastoplastic damage constitutive model for compressed asphalt mastic. *Journal of Central South University*, *21*, 4007−4013. doi:10.1007/s11771-014-2389-2

17. Dai Q.L., You Z.P. (2008): Micromechanical finite element framework for predicting viscoelastic properties of asphalt mixture. *Materials and Structures*, *41*, 1025-1037. doi:10.1617/s11527-007-9303-4

18. Dai Q.L. (2010): Micromechanical viscoelasto-plastic models and finite element implementation for rate-independent and rate-dependent permanent deformation of stone-based materials. *International Journal for Numerical and Analytical Methods in Geomechanics*, *34*, 1321-1345. doi:10.1002/nag.861

19. Zheng J.L., Lu S.T., Tian X.G. (2008): Viscoelastic damage characteristics of asphalt based on creep test (in Chinese). *Engineering Mechanics*, *25*, 193-196.

20. Voyiadjis G. Z. (2015). *Handbook of Damage Mechanics, Nano to Macro Scale for Materials and Structures.* 1st ed. Springer.

21. Liu J.Q., Li Q., Li H.X. (2014): A new creep model of asphalt mixture based on statistical damage theory. *Journal of Highway and Transportation Research and Development. (English Edition)* , *31*(8), 13-18.